Random transverse Ising spin chain and random walks

Ferenc Iglói
Research Institute for Solid State Physics, H-1525 Budapest, P.O. Box 49, Hungary
and Institute for Theoretical Physics, Szeged University, H-6720 Szeged, Hungary

Heiko Rieger
HLRZ, Forschungszentrum Jülich, 52425 Jülich, Germany
(Received 24 September 1997; revised manuscript received 26 November 1997)

We study the critical and off-critical (Griffiths-McCoy) regions of the random transverse-field Ising spin chain by analytical and numerical methods and by phenomenological scaling considerations. Here we extend previous investigations to surface quantities and to the ferromagnetic phase. The surface magnetization of the model is shown to be related to the surviving probability of an adsorbing walk and several critical exponents are exactly calculated. Analyzing the structure of low-energy excitations we present a phenomenological theory which explains both the scaling behavior at the critical point and the nature of Griffiths-McCoy singularities in the off-critical regions. In the numerical part of the work we used the free-fermion representation of the model and calculated the critical magnetization profiles, which are found to follow very accurately the conformal predictions for different boundary conditions. In the off-critical regions we demonstrated that the Griffiths-McCoy singularities are characterized by a single, varying exponent, the value of which is related through duality in the paramagnetic and ferromagnetic phases. [S0163-1829(98)03418-3]

I. INTRODUCTION

Magnetic systems with quenched disorder at very low or even vanishing temperature have attracted a lot of interest recently. In particular the quantum phase transition occurring in quantum Ising spin glasses in a transverse field[1] and random transverse Ising ferromagnets[2–4] turned out to have a number of surprising features. For instance, the presence of quenched disorder has more pronounced effects on quantum phase transitions than on those phase transitions, which are driven by thermal fluctuations. For example, in the Griffiths phase, which is at the disordered side of the critical point, the susceptibility has an essential singularity in classical systems, whereas in a random quantum system the corresponding singularity (Griffiths-McCoy singularity[5,6]) is much stronger, it is in a power-law form.

Many interesting features of random quantum systems can already be seen in one-dimensional models. After the pioneering work by McCoy and Wu[7] and later studies by Shankar and Murphy,[8] Fisher[2] has recently performed an exhaustive study of the critical behavior of the random transverse-field Ising spin chain. He used a renormalization-group (RG) approach, which he claims becomes exact at the critical point. The same type of method has later been used for other $1d$ random quantum problems[9] and recently some exact results are obtained through a mapping of the random XY model onto a Dirac equation in the continuum limit.[10]

In the present paper we consider the prototype of random quantum systems the random transverse-field Ising chain defined by the Hamiltonian:

$$H=-\sum_l J_l\sigma_l^x\sigma_{l+1}^x-\sum_l h_l\sigma_l^z. \tag{1.1}$$

Here the σ_l^x, σ_l^z are Pauli matrices at site l and the J_l exchange couplings and the h_l transverse fields are random variables with distributions $\pi(J)$ and $\rho(h)$, respectively. The Hamiltonian in Eq. (1.1) is closely related to the transfer matrix of a classical two-dimensional layered Ising model, which was introduced and studied by McCoy and Wu.[7]

In the following we briefly summarize the existing exact, conjectured, and numerical results on the random transverse-field Ising chain in Eq. (1.1). The quantum control parameter of the model is given by

$$\delta=\frac{[\ln h]_{\rm av}-[\ln J]_{\rm av}}{{\rm var}[\ln h]+{\rm var}[\ln J]}. \tag{1.2}$$

For $\delta<0$ the system is in the ordered phase with a nonvanishing average magnetization, whereas the region $\delta>0$ corresponds to the disordered phase. There is a phase transition in the system at $\delta=0$ with rather special properties, which differs in several respects from the usual second-order phase transitions of pure systems. One of the most striking phenomena is that some physical quantities are not self-averaging, which is due to very broad, logarithmic probability distributions. As a consequence the *typical value* (which is the value on an event with probability one) and the *average value* of such quantities is different. Thus the critical behavior of the system is primarily determined by rare events, dominating the averaged values of various observables.

The average surface magnetization close to the critical point vanishes as a power law $m_s\sim\delta^{\beta_s}$, where

$$\beta_s=1, \tag{1.3}$$

is an exact result by McCoy.[6] The average bulk magnetization is characterized by another exponent β, which is conjectured by Fisher in his RG treatment:[2]

$$\beta = 2 - \tau, \tag{1.4}$$

where $\tau = (1+\sqrt{5})/2$ is the golden mean. The average spin-spin correlation function $G(l) = [\langle \sigma_i^x \sigma_{i+l}^x \rangle]_{\rm av}$ involves the average correlation length ξ, which diverges at the critical point as $\xi \sim |\delta|^{-\nu_{\rm av}}$. The RG result by Fisher[2] is

$$\nu_{\rm av} = 2. \tag{1.5}$$

On the other hand, the typical correlations have a faster decay, since $\xi_{\rm typ} \sim |\delta|^{-\nu_{\rm typ}}$ with $\nu_{\rm typ} = 1$.[8]

In a quantum system statistics and dynamics are inherently connected. Close to the critical point the relaxation time t_r is related to the correlation length as $t_r \sim \xi^z$, where z is the dynamical exponent. The random transverse-field Ising spin chain is very strongly anisotropic at the critical point, since according to the RG picture[2] and to numerical results[11]

$$\ln t_r \sim \xi^{1/2}, \tag{1.6}$$

which corresponds to $z = \infty$. On the other hand, the relaxation time is related to the inverse of the energy-level spacing at the bottom of the spectrum $t_r \sim (\Delta E)^{-1}$. Then, as a consequence of Eq. (1.6) some energylike quantities (specific heat, bulk, and surface susceptibilities, etc.) have an essential singularity at the critical point, while the correlation function of the critical energy density has a stretched-exponential decay, in contrast to the usual power-law behavior.

Leaving the critical point towards the disordered phase the rare events with strong correlations still play an important role, until we reach the region $\delta > \delta_G$, where all transverse fields are bigger than the interactions. In the region $0 < \delta < \delta_G$, which is called the Griffiths-McCoy phase the magnetization is a singular function of the uniform longitudinal field H_x as $m_{\rm sing} \sim |H_x|^{1/z}$, where the dynamical exponent z varies with δ. At the two borders of the Griffiths-McCoy phase it behaves as $z \approx 1/2\delta(1+\mathcal{O}(\delta))^2$ as $\delta \to 0$ and $z = 1$ as $\delta \to \delta_G^-$, respectively.

Some of the above-mentioned results have been numerically checked[11] and in addition various probability distributions and scaling functions have been numerically determined.[12] Our present study, which contains analytical and numerical investigations extends the previous work in several respects. In the case of a limiting random distribution we obtain exact results on the surface magnetization exponent $x_s = \beta_s/\nu$ and in particular the thermal exponent ν through a simple directed walk consideration. The mapping of the problem of calculating various universal quantities for the random transverse Ising chain onto the calculation of statistical properties of appropriately defined random walks is one of the main achievements of the present paper. With its help we are also able to explain quantitatively many of the exotic features of the Griffiths-McCoy region on *both* sides of the transition.

Moreover, we improved the accuracy of the numerical estimates on the bulk magnetization exponent in Eq. (1.4). Furthermore we present results on the magnetization profiles in confined critical systems as well as about the probability distribution of several quantities.

Throughout the paper we use two types of random distributions. (1) The binary distribution, in which the couplings can take two values λ and $1/\lambda$ with the probability p and $q = 1-p$, respectively, while the transverse field is constant:

$$\pi(J) = p\,\delta(J-\lambda) + q\,\delta(J-\lambda^{-1}),$$

$$\rho(h) = \delta(h-h_0). \tag{1.7}$$

The critical point is given by $(p-q)\ln\lambda = \ln h_0$ and $\delta_G = \sqrt{p/q}$ for $\lambda < 1$. (2) The uniform distribution in which the couplings and the fields have uniform distributions:

$$\pi(J) = \begin{cases} 1, & \text{for } 0 < J < 1 \\ 0, & \text{otherwise} \end{cases}$$

$$\rho(h) = \begin{cases} h_0^{-1}, & \text{for } 0 < h < h_0 \\ 0, & \text{otherwise,} \end{cases} \tag{1.8}$$

and the critical point is at $h_0 = 1$ and $\delta_G = \infty$.

The structure of the paper is the following. In Sec. II we present the free-fermionic description of our model together with the way of calculation of several physical quantities in this representation. In Sec. III the surface magnetization and several critical exponents are calculated exactly using a correspondence with an adsorbing walk problem. Phenomenological considerations and numerical estimates about the distribution of low-energy excitations are compared in Sec. IV. Numerical results for different critical and off-critical parameters are presented in Secs. V and VI, respectively. Our results are discussed in the final section.

II. FREE-FERMION REPRESENTATION

We consider the random transverse-field Ising spin chain in Eq. (1.1) on a finite chain of length L with free or fixed boundary conditions, i.e., with $J_L = 0$. The Hamiltonian in Eq. (1.1) is mapped through a Jordan-Wigner transformation and a following canonical transformation[13] into a free-fermion model:

$$H = \sum_{q=1}^{L} \epsilon_q \left(\eta_q^+ \eta_q - \frac{1}{2} \right), \tag{2.1}$$

where η_q^+ and η_q are fermion creation and annihilation operators, respectively. The fermion energies ϵ_q are obtained via the solution of an eigenvalue problem, which necessitates the diagonalization of a $2L \times 2L$ tridiagonal matrix $\mathbf{T}$ with nonvanishing matrix elements $T_{2i-1,2i} = T_{2i,2i-1} = h_i$, $i = 1,2, \ldots, L$ and $T_{2i,2i+1} = T_{2i+1,2i} = J_i$, $i = 1,2, \ldots, L-1$. We denote the components of the eigenvectors V_q as $V_q(2i-1) = -\phi_q(i)$ and $V_q(2i) = \psi_q(i)$, $i = 1,2, \ldots, L$, i.e.,

$$\mathbf{T}=\begin{pmatrix} 0 & h_1 & & & & & \\ h_1 & 0 & J_1 & & & & \\ & J_1 & 0 & h_2 & & & \\ & & h_2 & 0 & \ddots & & \\ & & & \ddots & \ddots & J_{L-1} & \\ & & & & J_{L-1} & 0 & h_L \\ & & & & & h_L & 0 \end{pmatrix},$$

$$V_q=\begin{pmatrix} - & \Phi_q(1) \\ & \Psi_q(1) \\ - & \Phi_q(2) \\ & \vdots \\ & \Psi_q(L-1) \\ - & \Phi_q(L) \\ & \Psi_q(L) \end{pmatrix}. \tag{2.2}$$

One is confined to the $\epsilon_q \geqslant 0$ part of the spectrum.[14]

A. Magnetization

Technically the calculation is more simple, when the boundary condition (bc) does not break the symmetry of the Hamiltonian, therefore we start with a chain with two free ends. As a consequence, in this case the ground-state expectation value of the local magnetization operator $\langle 0|\sigma_l^x|0\rangle^{\text{free}}$ is zero for finite chains. Then the scaling behavior of the magnetization at the critical point is obtained from the asymptotic behavior of the (imaginary) time-time correlation function:

$$G_l(\tau)=\langle 0|\sigma_l^x(\tau)\sigma_l^x(0)|0\rangle = \sum_i |\langle i|\sigma_l^x|0\rangle|^2 \exp[-\tau(E_i-E_0)], \tag{2.3}$$

where $|0\rangle$ and $|i\rangle$ denote the ground state and the ith excited state of H in Eq. (2.1), with energies E_0 and E_i, respectively. In the thermodynamic limit in the ordered phase of the system the first excited state is asymptotically degenerate with the ground state, thus the sum in Eq. (2.3) is dominated by the first term. In the large τ limit $\lim_{\tau\to\infty} G_l(\tau)=m_l^2$, thus the local magnetization is given by the off-diagonal matrix element:

$$m_l^{\text{free}}=\langle 1|\sigma_l^x|0\rangle. \tag{2.4}$$

In the fermion representation the magnetization operator is expressed as

$$\sigma_l^x=A_1B_1A_2B_2 \ \ldots \ A_{l-1}B_{l-1}A_l \tag{2.5}$$

with

$$A_i=\sum_q \phi_q(i)(\eta_q^+ + \eta_q), \quad B_i=\sum_q \psi_q(i)(\eta_q^+ - \eta_q). \tag{2.6}$$

Using $|1\rangle=\eta_1^+|0\rangle$ the matrix element in Eq. (2.4) is evaluated by Wick's theorem. Since for $i\neq j$ $\langle 0|A_iA_j|0\rangle = \langle 0|B_iB_j|0\rangle = 0$ we obtain for the local magnetization

$$m_l^{\text{free}}=\begin{vmatrix} H_1 & G_{11} & G_{12} & \ldots & G_{1l-1} \\ H_2 & G_{21} & G_{22} & \ldots & G_{2l-1} \\ \vdots & \vdots & \vdots & \ddots & \vdots \\ H_l & G_{l1} & G_{l2} & \ldots & G_{ll-1} \end{vmatrix}, \tag{2.7}$$

where

$$H_j=\langle 0|\eta_1 A_j|0\rangle=\Phi_1(j),$$

$$G_{jk}=\langle 0|B_kA_j|0\rangle=-\sum_q \Psi_q(k)\Phi_q(j). \tag{2.8}$$

We note that the off-diagonal magnetization m_l^{free} in Eq. (2.4) can be used to study the scaling behavior of the critical magnetization through finite-size scaling.

Next we turn to consider the system with symmetry breaking bc's, when one of the boundary spins is fixed. Then one should formally put $h_1=0$ or $h_L=0$. For instance, if we fix the spin at site L we put $h_L=0$, implying that σ_L^x now commutes with the Hamiltonian and S_L^x is a good quantum number. In the fermionic description the twofold degeneracy of the energy levels, corresponding to $S_L^x=+1$ and $S_L^x=-1$, is manifested by a zero energy mode: $\varepsilon_1=0$ in Eq. (2.1), with an eigenvector which satisfies $V_1(2i)=\psi_1(i)=0$, $i=1,2,\ \ldots\ ,L$.[15] Then the first excited state $|1\rangle$ is degenerate with the ground state $|0\rangle$ and the matrix element in Eq. (2.4) corresponds to the *ground-state* expectation value of the magnetization

$$m_l^{\text{free}+}=\langle 0|\sigma_l^x|0\rangle, \tag{2.9}$$

which is formally given by the determinant in Eq. (2.7). The surface magnetization $m_s \equiv m_1=\phi_1(1)$ can be computed in a straightforward manner by simply solving the equation $\mathbf{T}V_1=0$ with $V_1(2i)=\psi_1(i)=0$ for $i=1,\ \ldots\ ,L$ and using the normalization condition $\Sigma_i \phi_1(i)^2=1$. This leads to the exact formula

$$m_s=\left[1+\sum_{l=1}^{L-1}\prod_{j=1}^{l}\left(\frac{h_j}{J_j}\right)^2\right]^{-1/2}, \tag{2.10}$$

which has been derived in Ref. 16 in the thermodynamic limit $L\to\infty$. Note that with the boundary condition considered here we proved that Eq. (2.10) is also exact for any *finite* system.

Next we consider those boundary conditions, when both boundary spins are fixed. Then one should formally put $h_1=0$ and $h_L=0$. This situation is, however, more complicated than the mixed bc, since it describes both parallel $(++)$ and antiparallel $(+-)$ boundary conditions. To determine the magnetization profiles in these cases we make use of the duality properties of the quantum Ising model. First we define the dual Pauli operators $\tau_{i+1/2}^x, \tau_{i+1/2}^z$ as

$$\tau_{i+1/2}^z=\sigma_i^x\sigma_{i+1}^x, \quad \sigma_i^z=\tau_{i-1/2}^x\tau_{i+1/2}^x, \tag{2.11}$$

in terms of which the Hamiltonian in Eq. (1.1) is expressed as

$$H=-\sum_l J_l\tau^z_{l+1/2}-\sum_l h_l\tau^x_{l-1/2}\tau^x_{l+1/2}. \tag{2.12}$$

In the dual model formally the couplings and fields are interchanged, thus the dual Hamiltonian has zero surface fields, since $J_0=J_L=0$ in Eq. (1.1). Then it can be easily shown that the even sector (i.e., those states which contain even number of fermions) of the free chain corresponds to the $(++)$ parallel boundary condition of the dual model, whereas the odd sector of the free chain to the $(+-)$ antiparallel boundary condition.

To obtain the magnetization profile for fixed boundary spin conditions we use the expression

$$\tau^x_{l+1/2}=\sigma^z_0\sigma^z_1\ \ldots\ \sigma^z_l, \tag{2.13}$$

which can be obtained from Eq. (2.11), then express the product of σ^z's by fermion operators through the relation $\sigma^z_i=A_iB_i$ and evaluate the right-hand side (rhs) of Eq. (2.13) in the corresponding free-chain situation. For the parallel spin boundary condition we take the free-chain vacuum expectation value:

$$m_l^{++}=\langle 0|\tau^x_{l+1/2}|0\rangle^{++}=\langle 0|A_0B_0A_1B_1\ \ldots\ A_lB_l|0\rangle^{\text{free}}, \tag{2.14}$$

which can be expressed through Wick's theorem as

$$m_l^{++}=\begin{vmatrix} 1 & 0 & 0 & \ldots & 0 \\ 0 & \widetilde{G}_{11} & \widetilde{G}_{12} & \ldots & \widetilde{G}_{1l} \\ \vdots & \vdots & \vdots & \ddots & \vdots \\ 0 & \widetilde{G}_{l1} & \widetilde{G}_{l2} & \ldots & \widetilde{G}_{ll} \end{vmatrix}. \tag{2.15}$$

Here $\widetilde{G}_{jk}$ is the same as in Eq. (2.8), however it is calculated with the dual couplings $h_l\leftrightarrow J_l$.

To obtain the magnetization profile in the antiparallel spin boundary condition $(+-)$ one should take the expectation value of the rhs of Eq. (2.13) in the lowest state of the odd sector of the free chain, which is the first excited state of the Hamiltonian: $|1\rangle=\eta_1^+|0\rangle$. Thus

$$m_l^{+-}=\langle 0|\tau^x_{l+1/2}|0\rangle^{+-}=\langle 1|A_0B_0A_1B_1\ \ldots\ A_lB_l|1\rangle^{\text{free}}. \tag{2.16}$$

To evaluate this expression by Wick's theorem one should notice that the state $|1\rangle=\eta_1^+|0\rangle$ can be considered the vacuum state of such a system, where η_1 and η_1^+ are interchanged, which formally means that $\psi_1(k)\rightarrow-\psi_1(k)$ and $\epsilon_1\rightarrow-\epsilon_1$. Then the expectation values in Eq. (2.8) are modified as

$$\overline{G}_{jk}=\langle 1|B_kA_j|1\rangle=-\sum_{q>1}\Psi_q(k)\Phi_q(j)+\Psi_1(k)\Phi_1(j), \tag{2.17}$$

which again have to be evaluated with the dual couplings $h_l\leftrightarrow J_l$. Then the m_l^{+-} profile is given by the determinant in Eq. (2.15), where the matrix elements $\widetilde{G}_{jk}$ are replaced by $\overline{G}_{jk}$.

B. Susceptibility and autocorrelations

The local susceptibility χ_l at site l is defined through the local magnetization m_l as

$$\chi_l=\lim_{H_l\rightarrow 0}\frac{\delta m_l}{\delta H_l}, \tag{2.18}$$

where H_l is the strength of the local longitudinal field, which enters in the Hamiltonian in Eq. (1.1) as $H_l\sigma^x_l$. χ_l can be expressed as

$$\chi_l=2\sum_i\frac{|\langle i|\sigma^x_l|0\rangle|^2}{E_i-E_0}, \tag{2.19}$$

which for boundary spins is simply given by

$$\chi_1=2\sum_q\frac{|\phi_q(1)|^2}{\epsilon_q}. \tag{2.20}$$

Next we consider the dynamical correlations of the system as a function of the imaginary time τ. First, we note that the correlations between surface spins can be obtained directly from Eq. (2.3) as

$$G_1(\tau)=\sum_q|\Phi_q(1)|^2\exp(-\tau\epsilon_q). \tag{2.21}$$

For bulk spins the matrix element $\langle i|\sigma^x_l|0\rangle$ in Eq. (2.3) is more complicated to evaluate, therefore one goes back to the first equation of Eq. (2.3) and considers the time evolution in the Heisenberg picture:

$$\begin{aligned}\sigma^x_l(\tau)&=\exp(\tau H)\sigma^x_l\exp(-\tau H)\\ &=A_1(\tau)B_1(\tau)\ \ldots\ A_{l-1}(\tau)B_{l-1}(\tau)A_l(\tau).\end{aligned} \tag{2.22}$$

The general time and position-dependent correlation function

$$\langle\sigma^x_l(\tau)\sigma^x_{l+n}\rangle=\langle A_1(\tau)B_1(\tau)\cdots A_l(\tau)A_1B_1\cdots A_{l+n}\rangle, \tag{2.23}$$

can then be evaluated by Wick's theorem as a product of two-operator expectation values, which in turn is written into the compact form as a Pfaffian:

$$\langle \sigma_l^x(\tau)\sigma_{l+n}^x\rangle = \begin{vmatrix} \langle A_1(\tau)B_1(\tau)\rangle & \langle A_1(\tau)A_2(\tau)\rangle & \langle A_1(\tau)B_2(\tau)\rangle & \cdots & \langle A_1(\tau)A_l(\tau)\rangle & \langle A_1(\tau)A_1\rangle & \cdots & \langle A_1(\tau)A_{l+n}\rangle \\ & \langle B_1(\tau)A_2(\tau)\rangle & \langle B_1(\tau)B_2(\tau)\rangle & \cdots & \langle B_1(\tau)A_l(\tau)\rangle & \langle B_1(\tau)A_1\rangle & \cdots & \langle B_1(\tau)A_{l+n}\rangle \\ & & \langle A_2(\tau)B_2(\tau)\rangle & \cdots & \langle A_2(\tau)A_l(\tau)\rangle & \langle A_2(\tau)A_1\rangle & \cdots & \langle A_2(\tau)A_{l+n}\rangle \\ & & & & \ddots & & & \vdots \\ & & & & & & & \langle B_{l+n-1}A_{l+n}\rangle \end{vmatrix}$$
$$= \pm[\det C_{ij}]^{1/2}, \tag{2.24}$$

where C_{ij} is an antisymmetric matrix $C_{ij}=-C_{ji}$, with the elements of the Pfaffian (2.24) above the diagonal. At zero temperature the elements of the Pfaffian are the following:

$$\langle A_j(\tau)A_k\rangle = \sum_q \Phi_q(j)\Phi_q(k)\exp(-\tau\epsilon_q),$$
$$\langle A_j(\tau)B_k\rangle = \sum_q \Phi_q(j)\Psi_q(k)\exp(-\tau\epsilon_q),$$
$$\langle B_j(\tau)B_k\rangle = -\sum_q \Psi_q(j)\Psi_q(k)\exp(-\tau\epsilon_q), \tag{2.25}$$
$$\langle B_j(\tau)A_k\rangle = -\sum_q \Psi_q(j)\Phi_q(k)\exp(-\tau\epsilon_q),$$

whereas the equal-time contractions are given in Eq. (2.6). For the finite-temperature contractions see Ref. 17.

III. SURFACE MAGNETIZATION AND THE MAPPING TO ADSORBING WALKS

In this section we analyze the surface magnetization of the RTIM (random transverse Ising model) using a mapping to an adsorbing random-walk problem. In this way we obtain exact results for the critical exponents β_s and ν, as well as for the surface magnetization scaling dimension x_m^s. These observations will then be used in the following section to identify the structure of the strongly coupled domains (SCD's), which are responsible for the low-energy excitations in the system.

A. Surface magnetization and correlation length

The surface magnetization in Eq. (2.10) represents perhaps the simplest order parameter of the transverse-field Ising chain. Note that the scaling behavior of end-to-end correlations

$$C_L=[\langle \sigma_1^x\sigma_L^x\rangle]_{\rm av} \tag{3.1}$$

is identical to that of the surface magnetization since C_L as well as m_s involve only surface spin operators that have anomalous dimension x_s. So, for instance, $C_L(\delta=0)\sim L^{-2x_s}$ and $C_{L\to\infty}(\delta)\sim\delta^{2\beta_s}$.

In the following we determine its average behavior for the symmetric binary distribution, i.e., with $p=q=1/2$ in Eq. (1.7). First we consider the system of a large, but finite length L at the critical point. In the limit $\lambda\to 0$ the surface magnetization in Eq. (2.10), which is expressed as a sum of products has a simple structure. Considering a random realization of the couplings the surface magnetization is zero, whenever a product of the form of $\Pi_{i=1}^{l} J_i^{-2}$, $l=1,2,\ldots,L$ is infinite, i.e., the number of λ couplings exceeds the number of λ^{-1} couplings in any of the $[1,l]$ intervals. On the other hand, if the surface magnetization has a finite value, it could be of the form $m_s=1/(n+1)^{1/2}$, where $n=0,1,2,\ldots$ measures the number of intervals, which are characterized by having the same number of λ and λ^{-1} couplings. To have a more transparent picture we represent the distribution of couplings by directed walks, which start at zero and make the ith steps upwards (for a coupling $J_i=\lambda^{-1}$) or downwards (for a coupling $J_i=\lambda$). As illustrated in Fig. 1 the surface magnetization corresponding to a random sequence is nonzero, only if the representing walk does not go below the ''time'' axis,[18] while the corresponding surface magnetization is given as $m_s=1/(n+1)^{1/2}$, where now n just counts the number of times the walk has touched the t axis for $t>0$.

Then the ratio of walks representing a sample with finite surface magnetization is just the survival probability of the walk $P_{\rm surv}$, which is given by $P_{\rm surv}(L)\propto L^{-1/2}$, for walks (samples) of length L. In the thermodynamic limit this probability vanishes, thus the *typical* realization of the chain, i.e., the event with probability one has zero surface magnetization. This is certainly different from the *average* value, which is dominated by the rare events represented by surviving walks with an $m_s=O(1)$. Consequently the average surface magnetization of a critical chain of length L is given by

$$[m_s(L,\delta=0)]_{\rm av}=AL^{-1/2}+O(L^{-3/2}). \tag{3.2}$$

On the other hand, one knows from finite-size scaling that $[m_s(L,\delta=0)]_{\rm av}\sim L^{-x_m^s}$, where $x_m^s=\beta_s/\nu$ is the scaling dimension of the surface magnetization. Thus from Eq. (3.2) we can read the *exact result*:

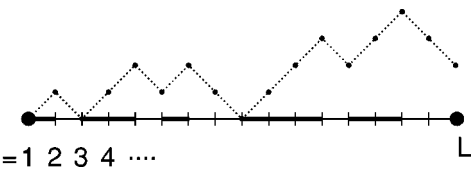

FIG. 1. Sketch of the correspondence between a bond configuration and a random walk. The thick segments in the horizontal line indicate strong ($J_i=\lambda^{-1}$) bonds, thin segments weak bonds ($J_i=\lambda$). This bond configuration corresponds to a surviving walk (as indicated by the broken line staying completely above the horizontal line), implying a finite surface magnetization. Actually for this example $m_s=1/3^{1/2}$ in the case $\lambda=0$, since the random walk touches the horizontal line three times (including the starting point).

$$x_m^s = \frac{1}{2}, \tag{3.3}$$

while the prefactor in Eq. (3.2) is obtained as $A = 0.643\,196\,1$ from a numerical calculation.

In the following we argue that the exponent in Eq. (3.3) is the same far all values λ of the binary distribution. First we mention that the finite-size critical surface magnetization $[m_s^\lambda(L,0)]_{\rm av}$ is a monotonically decreasing function of $\lambda \leqslant 1$: $[m_s^{\lambda_1}(L,0)]_{\rm av} < [m_s^{\lambda_2}(L,0)]_{\rm av}$ $0 \leqslant \lambda_1 < \lambda_2 \leqslant 1$ for any value of L. Thus the corresponding exponents also satisfy $x_m^s(\lambda_1) \leqslant x_m^s(\lambda_2)$. However according to exact results the value of x_m^s is the same, i.e., 1/2 for the homogeneous model[19] ($\lambda = 1$) and for the extreme inhomogeneous model ($\lambda \to 0$), thus the relation in Eq. (3.3) should hold for any parameters of the distribution. We note that this is the first exact derivation of the x_m^s exponent, the value of which is in agreement with previously known exact and conjectured results in Eqs. (1.3) and (1.5).

Next we calculate the ν exponent from the δ dependence of the surface magnetization. In the scaling limit $L \gg 1$, $|\delta| \ll 1$ the surface magnetization can be written as

$$[m_s^\lambda(L,\delta)]_{\rm av} = [m_s^\lambda(L,0)]_{\rm av} \widetilde{m}_s(\delta L^{1/\nu}). \tag{3.4}$$

Here the scaling function $\widetilde{m}_s(y)$, which depends on the ratio of L and the correlation length ξ, can be expanded as $\widetilde{m}_s(y) = 1 + By + O(y^2)$, so that one obtains for the δ correction to the surface magnetization:

$$[m_s(L,\delta)]_{\rm av} - [m_s(L,0)]_{\rm av} \propto \delta L^{\Theta}, \tag{3.5}$$

with $\Theta = 1/\nu - x_m^s$. This exponent can also be determined in the $\lambda \to 0$ limit of the binary distribution. Now, slightly outside the critical point the products of l terms in the sum of Eq. (2.10) will contain a factor of $(1+\delta)^{2l} \simeq 1 + 2l\delta$ in leading order of δ. Then the surface magnetization of a coupling distribution which is represented by a surviving walk is given by

$$m_s = \left[1 + \sum_{i=1}^{n} (1 + 2l_i\delta) \right]^{-1/2}$$

$$= (1+n)^{-1/2} - \delta \frac{\sum_i l_i}{(n+1)^{3/2}} + O(\delta^2), \tag{3.6}$$

where l_i gives the position of the ith touching point of the walk with the t axis. Next we consider a typical surviving walk, which has $n = O(1)$ return points (since the probability of n returns decreases exponentially), and these points are situated at $l_i = O(L^{1/2})$. Consequently for a typical surviving walk the correction term in Eq. (3.6) is $O(L^{1/2})$, which should be multiplied by the surviving probability of $O(L^{-1/2})$. Since the surviving walks have a sharp probability distribution we are left with the result: $[m_s(L,\delta)]_{\rm av} - [m_s^\lambda(L,0)]_{\rm av} = B\delta + O(\delta^2)$, where the constant is given from numerical calculations as: $B = 0.270\,563 \simeq 17/20\pi$. Comparing our result with that in Eq. (3.5) we get for the correlation length critical exponent

$$\nu = 2. \tag{3.7}$$

This is an exact determination of the exponent ν. We obtained it for a particular limit $\lambda \to 0$ for the binary distribution (1.7), which is a very broad distribution of couplings and therefore essentially the limit in which Fisher's RG analysis[2] becomes exact, too. *Cum grano salis* one might say that here we presented a way to perform exact calculation by using directly the fixed-point distribution occuring in this RG study.

B. Relation between surface magnetization and adsorbing random walks

Here we summarize and extend the mapping between the surface magnetization of the RTIM and the surviving probability of the corresponding adsorbing random walk. First, we consider again the extreme binary distribution of couplings in Eq. (1.7) with $h_0 = 1$, such that the control parameter in Eq. (1.2) is given by

$$\delta = \frac{q-p}{4pq} \frac{1}{\ln \lambda}. \tag{3.8}$$

Then, according to the considerations of the previous section, the corresponding adsorbing walk has an asymmetric character: it makes steps with probabilities p and $q = 1-p$ off and towards the wall, respectively. The corresponding control parameter $\delta_w = q - p$ in Eq. (A1) is proportional to δ in Eq. (3.8). Our basic observation can be summarized as

$$m_s(\delta, L) \sim P_{\rm surv}(\delta_w, L), \quad \delta \sim \delta_w. \tag{3.9}$$

At the critical point from Eq. (A7) $P_{\rm surv}(0,L) \sim L^{-\gamma}$ and $\gamma = 1/2$ is just x_m^s, the surface magnetization scaling dimension of the RTIM. *In the paramagnetic phase* of the RTIM $\delta > 0$ and the corresponding walk has a drift towards the adsorbing wall. The surviving probability in Eq. (A8)

$$P_{\rm surv}(\delta_w > 0, L) \sim \exp(-L/\xi_w),$$

$$\xi_w = \frac{8pq}{(p-q)^2} \sim \delta_w^{-2}, \tag{3.10}$$

is characterized by a correlation length, which diverges as $\xi_w \sim \delta^{-\nu}$ with $\nu = 2$. We note that the expression for ξ_w in Eq. (3.10) agrees with the RTIM result by Fisher.[2] Finally, *in the ferromagnetic phase* $\delta < 0$ the corresponding walk drifts off the wall and the surviving probability has a finite limit as $L \to \infty$:

$$P_{\rm surv}(\delta < 0, L \to \infty) = \frac{p-q}{p} \sim -\delta_w. \tag{3.11}$$

This expression then corresponds to a finite average surface magnetization of the RTIM, which linearly vanishes at the critical point. Thus the surface magnetization exponent of the RTIM is $\beta_s = 1$, in agreement with the exact results by McCoy.[6] The finite-size corrections to the surviving probability in Eq. (3.11) are exponential, according to Eq. (A10)

$$P_{\rm surv}(\delta < 0, L) - P_{\rm surv}(\delta < 0, L \to \infty) \sim \exp(-L/\xi_w), \tag{3.12}$$

with the correlation length ξ_w, as in Eq. (3.10). Consequently the ν critical exponent is the same below and above the transition point, as it generally should be.

These results obtained for the extreme binary distribution can be generalized for other random distributions, too. It is enough to notice that the surface magnetization in a sample with nonsurviving walk character is exponentially vanishing with the size of the system. Therefore the basic relation in Eq. (3.9) remains valid. Then at the critical point the $P_{\rm surv}(\delta=0,L)\sim L^{-1/2}$ is a consequence of the Gaussian nature of the random walk. Similarly, the relations $\xi_w\sim\delta_w^{-2}$, $\delta_w>0$ and $P_{\rm surv}(\delta_w<0,L)\sim-\delta_w$, $\delta_w<0$ follow from the scaling behavior of the random walks.

IV. DISTRIBUTION OF THE LOW-ENERGY EXCITATIONS

In the previous section we saw that the surface order is connected to a coupling distribution, which can be represented by a surviving walk. Since (local) order and small (vanishing) excitation energies are always connected, we can thus identify the local distribution of couplings, which results in a strongly coupled domain (SCD). Note that a SCD is not simply a domain of strong bonds, but it generally has a much larger spatial extent.[20]

To estimate the excitation energy ϵ of an SCD we make use the exact result for the lowest gap $\epsilon_1(l)$ of an Ising quantum chain of l spins with free bc:[21] Since we are interested in a bond and field configuration that gives rise to an exponentially small gap ϵ_1 we can neglect the rhs of the eigenvalue equation

$$\mathbf{T}\cdot V_1=\epsilon_1 V_1, \tag{4.1}$$

cf. Eq. (2.2) and derive approximate expressions for the eigenfunctions Φ_1 and Ψ_1. With these one arrives at

$$\epsilon_1(l)\sim m_s\overline{m}_s\cdot h_l\prod_{i=1}^{l-1}\frac{h_i}{J_i}. \tag{4.2}$$

Here m_s and $\overline{m}_s$ denote the finite-size surface magnetizations at both ends of the chain, as defined in Eq. (2.10) (for $\overline{m}_s$ simply replace h_j/J_j by h_{L-j}/J_{L-j} in this equation). If the sample has a low-energy excitation, then both end-surface magnetizations are of $O(1)$, consequently the coupling distribution follows a surviving walk picture. The corresponding gap estimated from Eq. (4.2) is given by

$$\epsilon_1\sim\prod_{i=1}^{l-1}\frac{h_i}{J_i}\sim\exp\{-l_{\rm tr}\cdot\overline{\ln(J/h)}\}, \tag{4.3}$$

where $l_{\rm tr}$ measures the size of transverse fluctuations of a surviving walk of length l and $\overline{\ln(J/h)}$ is an average coupling. In the following we assume that the excitation energy of surface SCD's are of the same order of magnitude as those localized in the bulk of the system and have the same type of coupling distributions. Thus we identify the SCD's, both at the surface and in the volume of the system, as a realization of couplings and fields with surviving walk character and having an excitation energy given in Eq. (4.3). With this prerequisite we are now ready to apply our theory for the critical and off-critical regions of the RTIM of L sites.

At the bulk critical point the characteristic length l of surviving regions is of the order of the size of the system L, thus the SCD extends over the volume of the system. The transverse fluctuations of the couplings in the SCD are from Eq. (A13) as $l_{\rm tr}\sim L^{1/2}$, thus we obtain for the scaling relation of the energy gap at the critical point:

$$\epsilon(\delta=0,L)\sim\exp(-\text{const}\cdot L^{1/2}), \tag{4.4}$$

in accordance with the existing numerical results.[11] At this point it is useful to point out the origin of the exponent 1/2 accompanying the length scale L in Eq. (4.4): it is the fact that the sequence of h_i/J_i is random and uncorrelated, for a general sequence one would have $l_{\rm tr}\sim L^{\omega}$ with ω being the wandering exponent (the scaling dimension of the transverse fluctuations) of the particular sequence under consideration. For instance one could also consider relevant aperiodic sequences (generated in a deterministic fashion), which have either the same or different wandering exponents, leading either to the same or a different scaling behavior of the energy scale at the critical point as the random chain studied here.[22]

In the paramagnetic phase the probability of finding a SCD of size l, which is localized at a given point is proportional to $\exp(-l/\xi)$, cf. Eq. (3.10). Since the SCD can be located at any point of the chain, the actual probability is proportional to the length of the chain, thus $P_L(l)\sim L\exp(-l/\xi)$. The characteristic size of SCD's obtained from the condition $P_L(l)=O(1)$ is given by

$$l\sim\xi\,\ln L,\quad \delta>0, \tag{4.5}$$

which grows very slowly with the linear size of the system. The characteristic transverse fluctuations of such a walk is given—according to Eq. (A16)—as $l_{\rm tr}\approx(q-p)l\alpha$, with $\alpha=O(1)$. Setting this expression into Eq. (4.3) we obtain the scaling relation

$$\epsilon(\delta>0,L)\sim L^{-z(\delta)}, \tag{4.6}$$

where the dynamical exponent $z(\delta)=2\alpha/\delta$ is a continuous function of the control parameter δ. Our estimate qualitatively agrees with Fisher's result,[2] that close to the critical point $z(\delta)=1/2\delta$.

The dynamical exponent $z(\delta)$ is conveniently measured from the scaling behavior of the probability distribution $P_L(l)\sim P_L(\ln(\epsilon))\sim L$. For a given large L the scaling combination from Eq. (4.6) is $L\epsilon^{1/z}$, thus

$$P(\epsilon)\sim\epsilon^{-1+1/z(\delta)}. \tag{4.7}$$

The distribution function of the gap in Eq. (4.7) has already been studied in Ref. 11 for periodic boundary conditions. Here we considered free chains and investigated the accumulated probability distribution

$$\Omega_L(\ln\epsilon)=\int_{-\infty}^{\ln\epsilon}dy\,P_L(y). \tag{4.8}$$

As seen in Fig. 2 the accumulated probability distribution for low energies is approximately a straight line on a log-log plot and from the slope one can estimate $1/z(\delta)$ quite accurately.

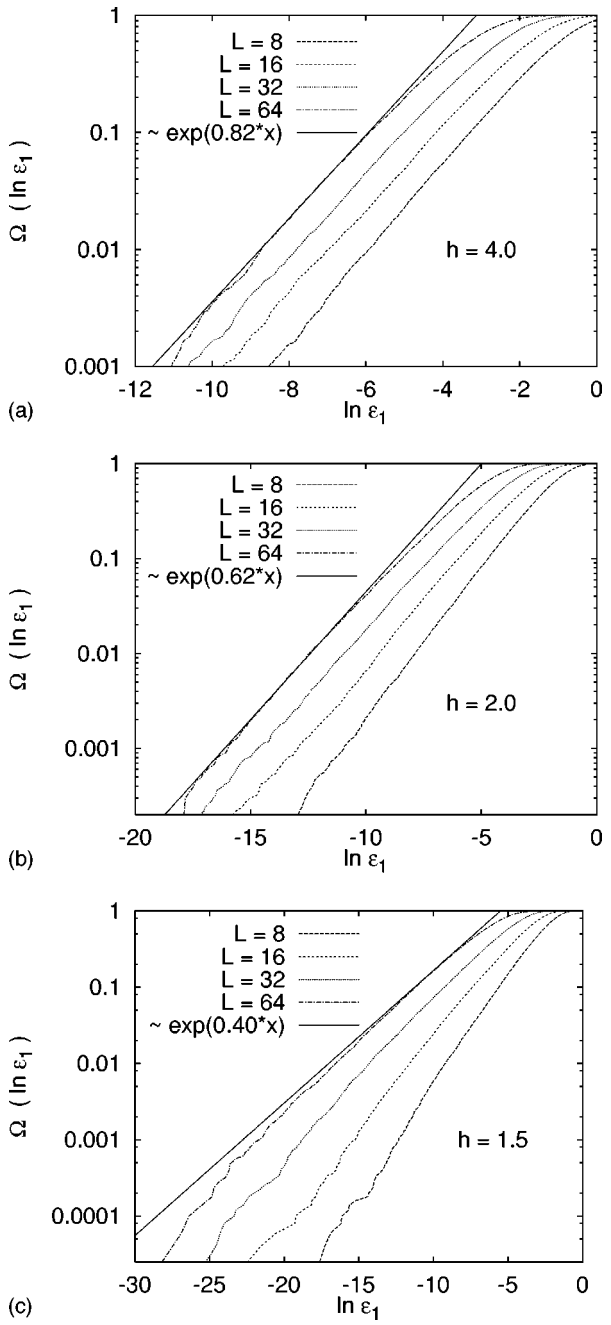

FIG. 2. The integrated gap probability distribution $\Omega_L(\ln \epsilon_1)$ in the disordered phase ($h>1$) for different values of h. The dynamical exponent $z(h)$ is extracted from the expected asymptotic form $\ln \Omega_L(\ln \epsilon_1)=1/z(h)(\ln \epsilon_1)+\text{const}$ which is a straight line when using a logarithmic scale on the y axes. Thus $1/z(h)\approx 0.82$, 0.62 and 0.40 for $h=4.0$, 2.0, and 1.5, respectively. The data for the uniform distribution averaged over 50 000 samples. Note that for large h, i.e., far away from the critical point, there is essentially no system size dependence, whereas closer to the critical point the asymptotic slope is reached only for large enough system sizes.

In the ferromagnetic phase of the RTIM the size of the SCD is of the order of the sample, $l\sim L$ and also the transverse fluctuations of the couplings are $l_{\rm tr}\sim L$. Consequently the energy of the first excitations scale exponentially with the size of the system: $\epsilon\sim\exp(-\text{const}L)$. Here, however, one should take into account that—due to the duality relation in Eq. (2.12)—in a strongly coupled environment there are always weakly coupled domains (WCD's), which are the counterparts of the SCD's in the paramagnetic phase. The characteristic size of a WCD is $O(\ln L)$, and their presence will reduce the size of the SCD's, such that one expects logarithmic corrections to the size of transverse fluctuations $l_{\rm tr}$. Indeed the numerical results on the accumulated gap distribution function in Fig. 3 can be interpreted with the presence of such corrections.

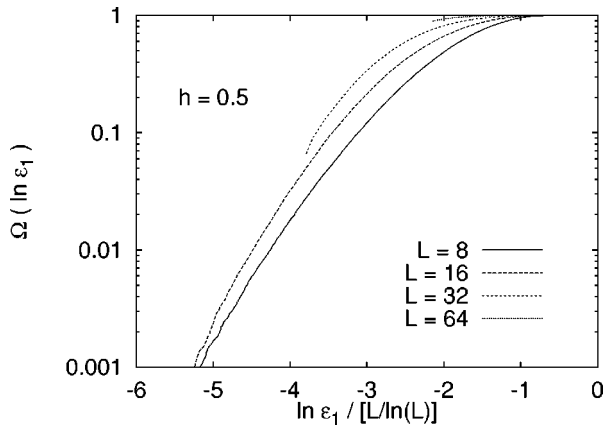

FIG. 3. The same as in the Fig. 2 in the *ordered* phase ($h<1$). The data do not scale with $\ln \epsilon_1/L$, there are strong logarithmic corrections. A scaling with $\ln \epsilon_1/[L/\ln(L)]$ is also poor (as can be seen in the figure), most probably higher powers of $\ln(L)$ are involved.

In the ferromagnetic phase many physical quantities (connected autocorrelation function, susceptibility, etc.) are connected with the distribution of the second gap. Unfortunately, we cannot make an estimate for ϵ_2 on the base of our present approach. However, our model is self-dual, the distributions of the couplings and the fields transform to each other in Eq. (2.12) for $\delta\rightarrow-\delta$. Therefore, we assume that the scaling behavior of ϵ_1 in the paramagnetic phase and that of ϵ_2 in the ferromagnetic phase are also related through duality, thus

$$\epsilon_2(\delta<0,L)\sim L^{-z(-\delta)}. \tag{4.9}$$

Indeed, as seen in Fig. 4 the scaling relation in Eq. (4.9) is satisfied, however with strong, logarithmic corrections.

V. CRITICAL PROPERTIES

A. Surface magnetization—canonical vs microcanonical ensemble

The surface magnetization of the RTIM has already been studied in Sec. III. Here we revisit this problem in order to answer the question, whether the values of the average quantities and the corresponding critical exponents depend or not on the ensemble used in the calculations. Our present study is motivated by a recent work[23] in which finite-size scaling methods and their predictions for critical exponents[24] have been scrutinized for random systems.

In our approach in Sec. III the bond and field configurations were taken completely random according to the corresponding distribution. We call this the *canonical* ensemble, since only the ensemble average of $\ln J_i$ and $\ln h_i$ is held fixed. One can also confine oneself on a subset of this en-

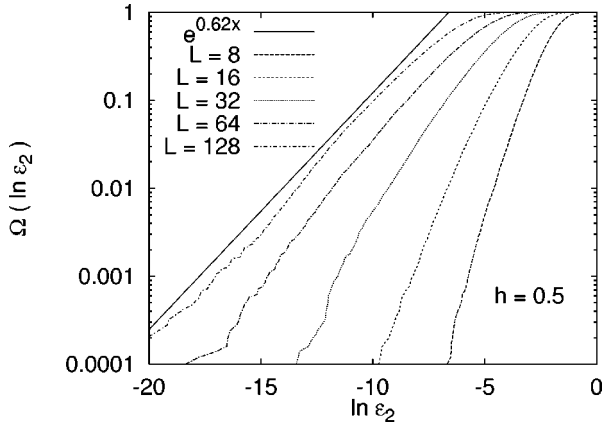

FIG. 4. The same as in Fig. 3 for the second lowest excitation, i.e., $\Omega_L(\ln \epsilon_2)$. One observes that asymptotically $\ln \Omega_L(\ln \epsilon_2) = 1/z(h) \ln \epsilon_2 + \text{const}$, with $z(h=0.5)=0.62=z(h=2.0)$ as one would expect from duality, by which $z(h)=z(1/h)$.

semble, in which we fix the value of the product of all bonds in the chain and similarly the product of all fields. Then the critical point of the system is exactly given by $\Sigma_{i=1}^{L-1} \ln J_i = \Sigma_{i=1}^{L-1} \ln h_i$, (note that we study the surface magnetization in a chain with one fixed boundary condition such that there are exactly as many bonds as fields). This we call the *microcanonical* ensemble. The motivation for the introduction of this ensemble can be found in Ref. 23: essentially it is a more restrictive way of fulfilling the criterium $[\ln J]_{\rm av} = [\ln h]_{\rm av}$ for being at the critical point.

The critical exponents of the canonical ensemble Eqs. (3.3), (1.5), which agree with other exact and RG results, are then the canonical ones.

We start to analyze the behavior of the surface magnetization in the paramagnetic phase ($\delta > 0$). In the microcanonical ensemble the product of the couplings and that of the fields are fixed, therefore the last term in the sum of Eq. (2.10) is of $\Pi_j (h_j/J_j)^2 \sim \exp(2\delta L)$, for each realizations. As a consequence the surface magnetization of the samples contains a prefactor $\exp(-\mathcal{A}\delta L)$, which is also present in the average value. It is easy to see that the leading finite-size dependence of the surface magnetization of *typical samples* is related to the above term and given by

$$[m_s(L, \delta > 0)]_{\rm typ}({\rm mc}) \sim \exp(-\mathcal{A}\delta L). \tag{5.1}$$

Thus in the microcanonical ensemble there are no rare events with $O(1)$ surface magnetizations and therefore the scaling behavior of the *average* and *typical* values are identical and for $\delta > 0$ we have the scaling combination δL.

In the canonical distribution, due to fluctuations in the product of the couplings, there are rare events with $O(1)$ surface magnetizations and their fraction $\exp(-\mathcal{A}\delta^2 L)$ in Eq. (3.10) governs the finite-size scaling behavior of the *average* surface magnetization, yielding $\nu_{\rm av}=2$. On the other hand, the *typical* behavior in the canonical ensemble is the same as in the microcanonical ensemble, see Eq. (5.1), by which $\nu_{\rm typ}=1$.

In the ferromagnetic phase ($\delta < 0$) the fraction of realizations with finite surface magnetization can be estimated as follows in the microcanonical ensemble. After $l < L$ steps the walk has an average drift of $l_{\rm dr} = -\delta_w l$, which exceeds the size of transverse fluctuations, $l_{\rm tr} \sim l^{-1/2}$, if $l > l_c \sim \delta_w^{-2}$. Therefore a walk which has been survived up to l_c steps with a probability of $P_{\rm surv} \sim l_c^{-1/2} \sim -\delta_w$ will not be adsorbed with probability of $O(1)$ in the following steps $l_c < l < L$. From this argument the microcanonical surface magnetization has a linear δ dependence close to the critical point, therefore the surface magnetization exponent

$$\beta_s({\rm mc}) = 1, \tag{5.2}$$

is the same as in the canonical distribution Eq. (1.3).

We can easily estimate the finite-size corrections to the surface magnetization in the ferromagnetic phase by noticing that the corrections to the surviving probability of the corresponding walk are proportional to the probability that the walk has a transverse fluctuation of the size of the drift $l_{\rm tr} \sim \delta_w L$, which is given by $\exp(-\mathcal{B} l_{\rm tr}^2/L\sigma^2) \sim \exp(-\mathcal{B}' L \delta_w^2)$. Consequently the finite-size corrections to the surface magnetization are given by $\exp(-L/\xi)$, with $\xi \sim \delta^{-2}$. Thus the correlation length exponent in the ordered phase is

$$\nu({\rm mc}) = 2, \quad \delta < 0, \tag{5.3}$$

which agrees with the canonical result in Eq. (3.7). We note that the above arguments about the surviving probability of random walks for $\delta < 0$ essentially hold for the canonical distribution, as a consequence the ferromagnetic phase of the RTIM has the same type of description in the two ensembles.

At the critical point of the model we use again the symmetric binary distribution in Eq. (1.7), such that the samples have the same number of λ and λ^{-1} couplings. In the extreme limit $\lambda \to 0$, as in the canonical case, the critical point surface magnetization can be determined exactly, through studying the surviving probability of the corresponding adsorbing random walk. To determine the microcanonical surviving probability first we note that from the canonical walks only a fraction of $O(L^{-1/2})$ is microcanonical. Second, the microcanonical surviving walks have their end at the starting point. Such returning surviving walks are of a fraction of $O(L^{-3/2})$ among the canonical walks. Thus the surviving probability of microcanonical walks is $P_{\rm surv}({\rm mc}) \sim L^{-1}$, therefore the microcanonical surface magnetization satisfies the scaling relation:

$$[m_s(L, \delta = 0)]_{\rm av}({\rm mc}) \sim L^{-1}. \tag{5.4}$$

The scaling combination between L and $\delta > 0$ is again obtained by analyzing the expression in Eq. (3.6). The typical number of return points of the surviving walks is again $n = O(1)$, but now $l_i = O(L)$, since the endpoint of the walk is a return point. Consequently, the correction term in Eq. (3.6) for surviving walks is $O(L)$, what should be multiplied by the surviving probability to obtain the average of $O(1)$, from which the scaling combination $L\delta$, $\delta > 0$ follows, in agreement with the previous determination below Eq. (5.1).

To summarize, the average surface magnetization of the RTIM has anomalous scaling behavior in the microcanonical ensemble: in Eq. (5.1) there is an exponentionally vanishing prefactor $\exp(-\mathcal{A}\delta L)$, which governs the scaling behavior of the surface magnetization in the paramagnetic phase. We note that in scaling theory the different scaling behavior in the low- and high-temperature phases is generally attributed

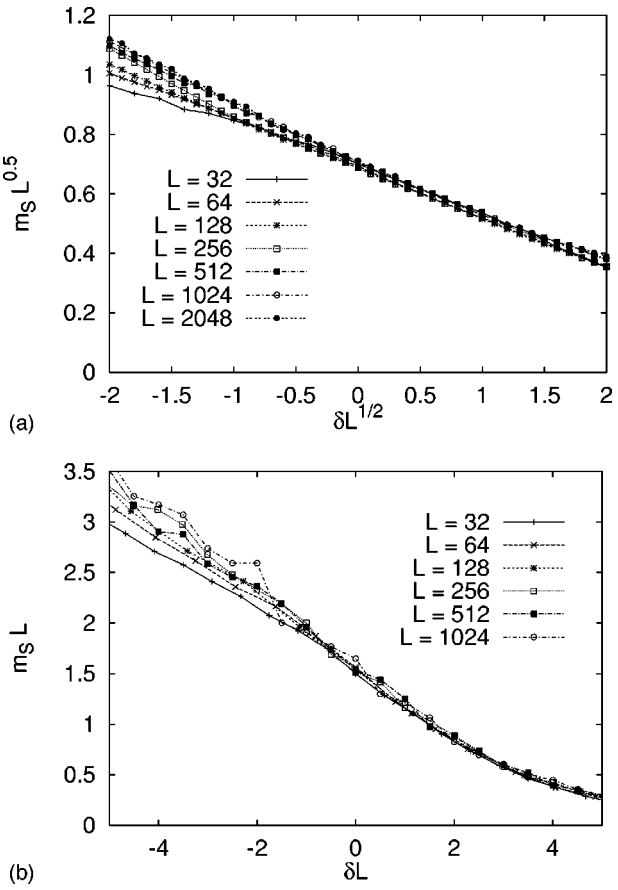

FIG. 5. Scaling plot of the surface magnetization in the canonical ensemble (top) and the microcanonical (bottom) ensemble. Both data are for the binary distribution (with $\lambda = 0.1$ averaged over 100 000 samples). Note that in the microcanonical ensemble scaling with δL is expected to hold for $\delta > 0$, but *not* for $\delta < 0$, cf. Eq. (5.3).

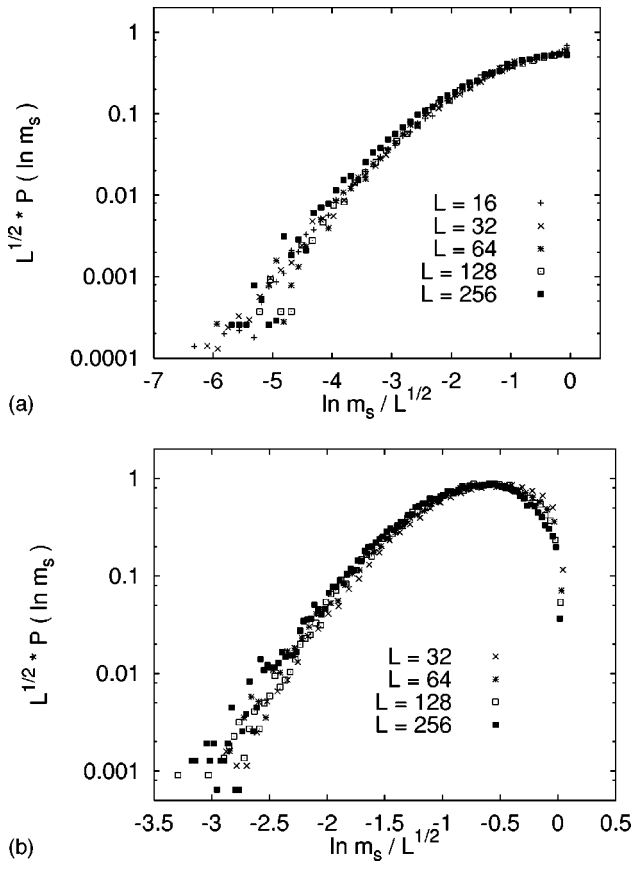

FIG. 6. Scaling plot of the probability distribution $P(\ln m_s)$ of the surface magnetization in the canonical ensemble (top) and the microcanonical (bottom) ensemble. Both data are for the uniform distribution averaged over 500 000 samples.

to the presence of a dangereous irrelevant scaling variable, see Ref. 25. In Fig. 5 we show the scaling plots for the surface magnetization in the two ensembles obtained numerically by evaluating Eq. (2.10) for the binary distribution. Note that we expect similar results to hold for end-to-end correlations $[\langle \sigma_1^x \sigma_L^x \rangle]_{\rm av}$, with the exponent x_s replaced by $2x_s$ (cf. Sec. III).

Another reason for the difference in the scaling behavior for $\delta > 0$ measured in the two ensembles is the fact that several physical quantities, among those the surface magnetization, is *not self-averaging* at the critical point. To illustrate this property in Fig. 6 we have plotted the probability distribution of the surface magnetization in the two ensemles. Both scale, as expected, as

$$P_L(\ln m_s) = \frac{1}{\sqrt{L}} \tilde{p}\left(\frac{\ln m_s}{\sqrt{L}} \right) \tag{5.5}$$

the asymptotic form of the scaling function $\tilde{p}$ for the canonical ensemble was determined analytically,[2] for particular distributions of the fields and/or couplings it can even be calculated exactly.[26]

The average is determined by the rare events having a magnetization of order $O(1)$, i.e., by the asymptotic behavior of $\tilde{p}(y)$ for $y \to 0$. From Fig. 5 (top) we conclude that for the canonical ensemble $\tilde{p}(y)$ approaches a constant for $y \to 0_-$, whereas for the microcanonical ensemble in Fig. 5 (bottom) the scaling functions shows a power-law dependence

$$\tilde{p}(y) \sim (-y)^a \quad \text{for } y \to 0_- \tag{5.6}$$

with a *positve* exponent a. For the average then follows

$$[m_s]_{\rm av} = \frac{1}{\sqrt{L}} \int dm \tilde{p}(\ln m_s / \sqrt{L})$$

$$\sim \frac{1}{\sqrt{L}} \int dm (|\ln m_s| / \sqrt{L})^a \propto L^{-(1+a)/2}. \tag{5.7}$$

As we said above $a = 0$ for the canonical ensemble, resulting in $[m_s]_{\rm av} \sim 1/\sqrt{L}$, and $a = 1$ fits the data reasonably well in case of the microcanonical ensemble, resulting in $[m_s]_{\rm av} \sim 1/L$.

Based on our observation on the surface magnetization we assume that for other non-self-averaging quantities the corresponding critical behavior could be anomalous in the microcanonical ensemble. In the rest of the paper we restrict ourselves to the canonical ensemble.

B. Profiles of observables

A real system is always geometrically constrained and due to modified surface couplings its properties in the surface region are generally different from those in the bulk. Close to the critical point this surface region, which has a characteristic size of the correlation length, intrudes far into the system. At the very critical point the appropriate way to describe the position-dependent physical quantities is to use density profiles rather than bulk and surface observables. For a number of universality classes much is known about the spatially inhomogeneous behavior, in particular in two dimensions, where conformal invariance provides a powerful tool to study various geometries.[27]

In a critical system confined between two parallel plates, which are at a large, but finite distance L apart, the local densities $\Phi(r)$ such as the order parameter (magnetization) or energy density vary with the distance l from one of the plates as a smooth function of l/L. According to the scaling theory by Fisher and de Gennes[28]

$$\langle \Phi(l) \rangle_{ab} = L^{-x_\Phi} F_{ab}(l/L), \tag{5.8}$$

where x_Φ is the bulk scaling dimension of the operator Φ, while ab denotes the boundary conditions at the two plates. In a d-dimensional system the scaling function in Eq. (5.8) has the asymptotic behavior:

$$F_{ab}(l/L) = A\left[1 + B_{ab}\left(\frac{l}{L}\right)^d + \ \ldots\ \right] \quad \frac{l}{L} \ll 1. \tag{5.9}$$

Here the amplitude of the first correction term is universal, the corresponding exponent is just $x_\Phi^s = d$ the surface scaling dimension of Φ.

In two dimensions conformal invariance gives further predictions on the profile:

$$\langle \Phi(l) \rangle_{ab} = \left[\frac{L}{\pi} \sin\ \pi \frac{l}{L}\right]^{-x_\Phi} G_{ab}(l/L), \tag{5.10}$$

where the scaling function $G_{ab}(l/L)$ depends on the universality class of the model and on the type of the boundary condition. With symmetric boundary conditions the scaling function is constant $G_{aa} = A$. For conformally invariant, nonsymmetric boundary conditions the scaling function has been predicted for several models. For the Ising model the magnetization profiles with free-fixed $(f+)$ and $(+-)$ boundary conditions are predicted as

$$G_{f+} = A\left[\sin \frac{\pi l}{2L}\right]^{x_m^s}, \tag{5.11}$$

and

$$G_{+-} = A\ \cos \frac{\pi l}{L}, \tag{5.12}$$

respectively.

In two dimensions conformal invariance can also be used to predict the critical off-diagonal matrix-element profiles $\langle \Phi | \Phi(l) | 0 \rangle$, where $\langle \Phi |$ denotes the lowest excited state leading to a nonvanishing matrix element [see Eq. (2.4)]. These off-diagonal profiles give information about the surface and bulk critical behavior via finite-size scaling, while avoiding the contribution of regular terms. With symmetric boundary conditions one obtains for the profile[29]

$$\langle \Phi | \Phi(l) | 0 \rangle \propto \left(\frac{\pi}{L}\right)^{x_\phi} \left(\sin\ \pi \frac{l}{L}\right)^{x_\Phi^s - x_\Phi}, \tag{5.13}$$

which involves both the bulk and surface scaling dimensions.

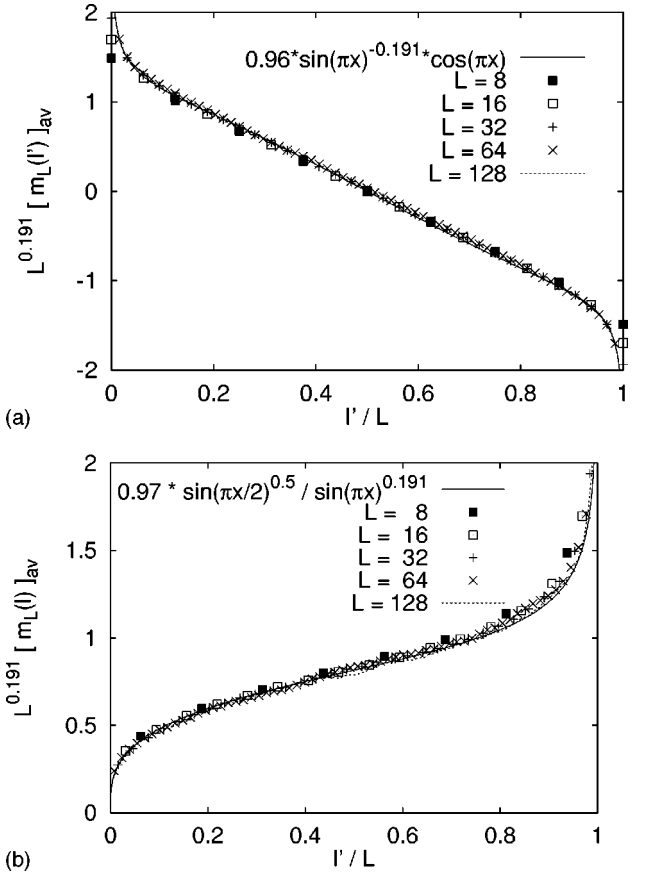

FIG. 7. Scaling plots of the magnetization profiles for nonsymmetric boundary conditions ($l' = l - 0.5$). Top: plus-minus $(+-)$ bc, the broken line is a fit to the form (5.10) and (5.12) with A as a fit parameter. Bottom: free-fixed $(f+)$ bc., the broken line is a fit to the form (5.10) and (5.11) with A as a fit parameter.

The numerically calculated average diagonal and off-diagonal magnetization profiles (see Sec. II) for the RTIM are presented in Figs. 7 and 8 for the uniform distribution (in Ref. 30 some data for the binary distribution have been presented). Here we do not use x_m and x_m^s as fit parameters, but fix them to the theoretically predicted values in Eqs. (1.4), (3.3). The only fit parameter is the nonuniversal prefactor A, which is found remarkably constant for the different boundary conditions. As one can see on Fig. 7 the data for different length L collapses to scaling curves, which are very well described by the scaling functions predicted by conformal invariance. Thus we can conclude that not only the scaling prediction by Fisher and de Gennes[28] in Eq. (5.8) is very well satisfied for the RTIM, but the corrections to the appropriate conformal results are also very small, practically negligible. This is an unexpected result, since the RTIM is not conformally invariant, due to anisotropic scaling at the critical point Eq. (1.6).

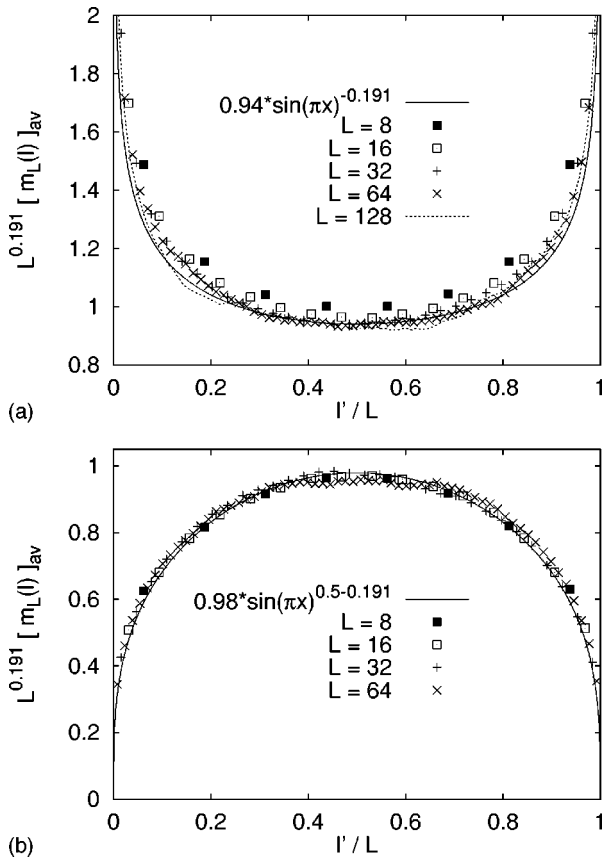

FIG. 8. Top: scaling plot of the magnetization profile for symmetric (here: fixed) boundary conditions. The broken line is a fit to the form (5.10) and $G_{aa}=A$ with A as a fit parameter. Bottom: the profile of the off-diagonal matrix element with free bc. The broken line is a fit to the form (5.13).

To close this section we present numerical results for the bulk magnetization scaling dimension x_m and compare it with Fisher's perhaps most striking prediction in Eq. (1.4). Here we have made effort to increase the numerical accuracy, therefore we worked with the binary distribution in Eq. (1.7) on chains with both ends fixed with length $L\leqslant 24$ and performed the *exact average* of the local magnetization on the central spin. From the finite-lattice magnetizations, which scales as $[m(L,0)]_{\rm av}\sim L^{-x_m}$ we have determined x_m by a two-point fit, comparing systems with sizes L and $L-2$. From the finite-size exponents, presented in Table I for $\lambda=2$, 3, and 4 one concludes that they are in agreement with Fisher's result: $x_m=(3-\sqrt{5})/4=0.191$. Unfortunately the numerical data in Table I show log-periodic oscillations, which are a consequence of the energy scale introduced by the binary distribution. Therefore one cannot use the accurate sequence-extrapolation methods to analyze the limiting behavior of the series. Instead, from a simple linear fit one can obtain the estimate

$$x_m=0.190\pm 0.003, \tag{5.14}$$

improving the accuracy of previous MC estimates.[11]

C. Dynamical correlations

The general time- and position-dependent correlations in Eq. (2.23) have a complicated structure at the critical point.

TABLE I. Numerical estimates for the bulk magnetization exponent $x_m(L)$ for the binary distribution for various values of λ.

	$x_m(L)$		
L	$\lambda=2$	$\lambda=3$	$\lambda=4$
6	0.127071	0.162136	0.181770
8	0.142310	0.161044	0.169656
10	0.157063	0.179177	0.189815
12	0.167197	0.195090	0.207268
14	0.173605	0.197072	0.206820
16	0.176458	0.196602	0.204265
18	0.178444	0.195288	0.201673
20	0.179836	0.194391	0.199992
22	0.181044	0.194279	0.199270
24	0.182175		

Therefore we consider dynamical correlations on the same spin, which has a simpler asymptotic behavior. First we consider the bulk autocorrelation function

$$G(\tau)=[\langle\sigma^x_{L/2}(\tau)\sigma^x_{L/2}\rangle]_{\rm av} \tag{5.15}$$

and recapitulate the scaling argument in Ref. 31.

The autocorrelation function, like the (local) magnetization, is not self-averaging at the critical point: its average value is determined by the *rare events*, which occur with a probability P_r, and P_r vanishes in the thermodynamic limit. In the random quantum systems the disorder is strictly correlated along the time axis, consequently in the rare events with a local order, i.e., with a finite magnetization also the autocorrelations are nonvanishing. Under a scaling transformation, when lengths are rescaled as $l'=l/b$, with $b>1$ the probability of the rare events transforms as $P_r'=b^{-x_m}$, like the local magnetization. As we said above the same is true for the autocorrelation function

$$G(\ln\,\tau)=b^{-x_m}G(\ln\,\tau/b^{1/2})\quad \delta=0, \tag{5.16}$$

where we have made use of the relation between relevant time t_r and length ξ at the critical point in Eq. (1.6). Taking now the length scale as $b=(\ln\,\tau)^2$ we obtain

$$G(\tau)\sim(\ln\,\tau)^{-2x_m}\quad \delta=0. \tag{5.17}$$

For surface spins in Eqs. (5.16), (5.17) the surface magnetization scaling dimension x_m^s appears.

In Fig. 9 we present the numerical results for the critical bulk autocorrelation function obtained via evaluating the Pfaffian Eq. (2.24). Note that we have chosen L to be odd, so that $L/2$ denotes the central spin, representing the bulk behavior in a system with free bc. A plot of $G(\tau)^{-1/2x_m}$, with x_m as in Eq. (5.14), versus $\ln\,\tau$ (or τ on a logarithmic scale) should yield a straight line in the infinite system size limit according to Eq. (5.17). As can be seen in Fig. 9 the data agree well with this prediction. For the surface autocorrelations $G_1(\tau)=[\langle\sigma^x_1(\tau)\sigma^x_1\rangle]_{\rm av}$, evaluated according to Eq. (2.21), which is much less involved than the computation of a Pfaffian, a similar plot with the bulk magnetization exponent x_m replaced by the surface magnetization exponent x_m^s gives also an excellent agreement with the prediction $G_1(\ln\,\tau)\sim(\ln\,\tau)^{-2x_m^s}$.

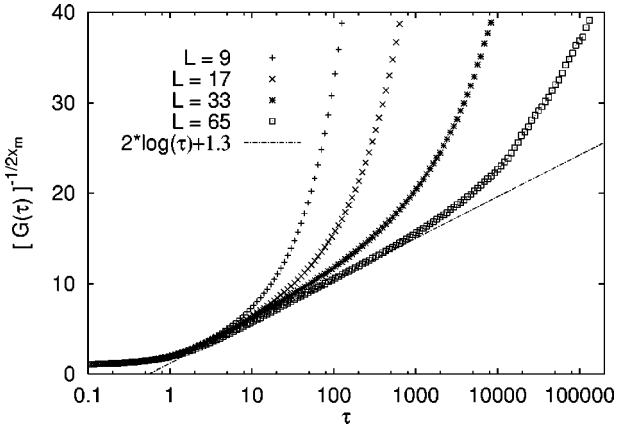

FIG. 9. Bulk spin-spin autocorrelation function $G(\tau)$ Eq. (5.15) for various system sizes (and the uniform distribution). The straight line is the prediction according to Eq. (5.17).

To complete the results on critical dynamics we mention the scaling behavior of the autocorrelation function $[\langle \sigma_l^z(\tau)\sigma_l^z\rangle]_{\rm av}$. We mention that σ_l^z represents one part of the local energy operator, the other part of which—$\sigma_l^x\sigma_{l+1}^x$—is related to it through duality. As shown in Ref. 31 this quantity at the critical point can be characterized by a power-law asymptotic decay with novel critical exponents, which are different in the bulk and at the surface of the system.

VI. OFF-CRITICAL PROPERTIES

A surprising property of random quantum systems is the existence of Griffiths-McCoy singularities in the paramagnetic side of the critical point. In the corresponding Griffiths-McCoy region the autocorrelation function decays as a power $G(\tau)\sim\tau^{-1/z(\delta)}$, where the dynamical exponent $z(\delta)$ characterizes also the distribution of low-energy excitations in Eq. (4.7). As a consequence, the free energy is a nonanalytic function of the magnetic field and the susceptibility diverges in the whole region.

According to the phenomenological theory[11] in the Griffiths-McCoy region the singularities of all physical quantities are entirely characterized by the dynamical exponent $z(\delta)$. Numerical calculations[11,12] give support to this assumption, although there are discrepancies between the values of $z(\delta)$ obtained from different quantities.

Here we extend previous investigations in several respects. First, we consider also the surface properties, such as the surface autocorrelation function and the surface susceptibility. Second, we investigate also the *ferromagnetic side* of the critical point. In the neighborhood of the critical point Fisher[2] has already obtained some RG results in the ferromagnetic phase. Here we are going to check these results numerically and to extend them for finite $\delta<0$.

A. Phenomenological scaling considerations

As already shown in Sec. IV the dynamical exponent $z(\delta)$ is conveniently measured from the probability distribution of the energy gap (in the ferromagnetic phase one considers the second gap in a finite system, which does not vanish exponentially). For large systems the gap distribution is given by Eq. (4.7) and with this the average autocorrelation function is given by

$$G(\tau)\sim\int_0^\infty P(\epsilon)\exp(-\tau\epsilon)d\epsilon\sim\tau^{-1/z(\delta)}. \tag{6.1}$$

In a finite system of size L for long enough time, such that $\tau\gg L^{z(\delta)}$, the decay in Eq. (6.1) will change to a $G(\tau)\sim 1/\tau$ form, which is characteristic for isolated spins. It means that in the above limit the system can be considered as an effective single spin.

In the following we present a simple scaling theory which explains the form of the asymptotic decay in Eq. (6.1). Here in the Griffiths-McCoy phase we modify the scaling relation in Eq. (5.16) by two respects. First, the scaling combination is changed to τ/b^z, since the dynamical exponent $z(\delta)$ is finite in the off-critical region. Second, the *rare events*, which are responsible for the Griffiths-McCoy singularities are now samples with very low-energy gaps and their number is practically independent of the size of the system. Consequently the rescaling prefactor is b^{-1} and the scaling relation is given by

$$G(\tau,1/L)=b^{-1}G(\tau/b^z,b/L)\quad \delta\neq 0, \tag{6.2}$$

where the inverse size of the system $1/L$ is also included as a scaling field. Now taking $b=\tau^{1/z}$ we obtain

$$G(\tau,1/L)=\tau^{-1/z}\widetilde{G}(\tau^{1/z}/L)\quad \delta\neq 0, \tag{6.3}$$

thus in the thermodynamic limit we recover the power-law decay in Eq. (6.1). The scaling function $\widetilde{G}(y)$ in Eq. (6.3) should behave as $\widetilde{G}(y)\sim y^{1-z}$ for large y, in this way one recovers the limiting $1/\tau$ decay, as argued below Eq. (6.1). Then the finite-size scaling behavior of the autocorrelation function is of the form of L^{z-1}, and after integrating $G(\tau,1/L)$ by τ the same scaling behavior will appear in the local susceptibility:

$$\chi_i(L)\sim L^{z-1},\quad \delta\neq 0. \tag{6.4}$$

B. Numerical calculation of the dynamical exponent

The phenomenological description of the Griffiths phase suggests that all Griffiths-McCoy singularities emerging in temperature, energy, time- or frequency-dependent quantities should be parametrizable by a single dynamical expontent $z(\delta)$. In this subsection we present the results on our numerical estimates for $z(\delta)$ resulting from the calculation of the following quantities:

(i) distribution of low-energy excitations,
(ii) autocorrelation function on bulk and surface spins,
(iii) distribution of surface susceptibilities.

The distribution functions for the energy gaps have already been presented in Sec. IV. The same quantity for the surface susceptibility in Eq. (2.20) has a similar form as the inverse gap, as seen in Fig. 10. The only difference that for the susceptibility the matrix element in the denominator of Eq. (2.20) select one special position of the SCD. As a consequence the corresponding probability distribution has no L

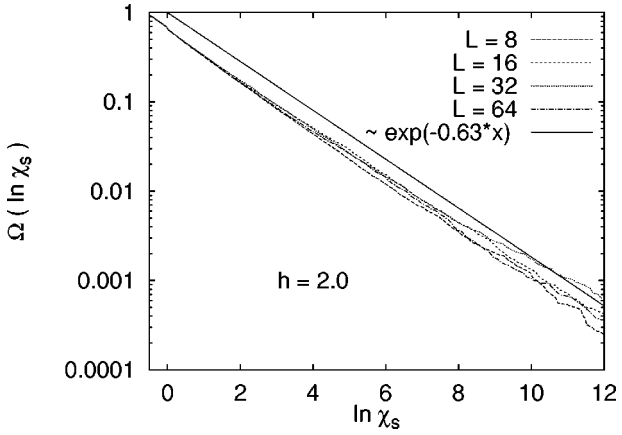

FIG. 10. Integrated probability distribution of the zero-frequency surface susceptibility for different system sizes in the disordered phase at $h=2.0$. Note that $z(h)$, as determined from the slope of the straight line, turns out to be within the error margin of $z(h)$ determined via the gap distribution (see Fig. 2).

dependence, as already discussed in Ref. 11 and can also be seen by comparing Eqs. (4.6) with (6.4). The $z(\delta)$ exponents calculated from the surface susceptibility distribution agree well with those obtained from the gap distribution.

The average autocorrelation function is measured at two sites of the chain: on the central spin, giving an estimate for the bulk correlation function and on the surface spin. The average bulk autocorrelation functions are drawn on a log-log plot in Fig. 11 for several values of $\delta>0$. One can easily notice an extended region of the curves, which are well approximated by straight lines, the slope of which is connected to the dynamical exponent through Eq. (6.1). Similar behavior can be seen in Fig. 12, where the average surface autocorrelation functions are drawn. Our investigation on the dynamical exponent is completed by studying the *connected* surface autocorrelation function in the ferromagnetic phase. As seen in Fig. 13 the scaling form in Eq. (6.1) is well satisfied for this function, too.

The behavior of the dynamical exponents calculated by different methods are summarized in Fig. 14. First we note that the numerical estimates are very close to each other. The only exception is the data obtained from the bulk autocorrelations. To explain the possible origin of this discrepancy we turn to Sec. VII. The $z(\delta)$ values well satisfy the two theoretical limits: $\lim_{|\delta|\to\infty} z(\delta)=1$ and $\lim_{|\delta|\to 0}=1/2\delta^2$. Furthermore the dynamical exponents show the duality relation: $z(\delta)=z(-\delta)$.

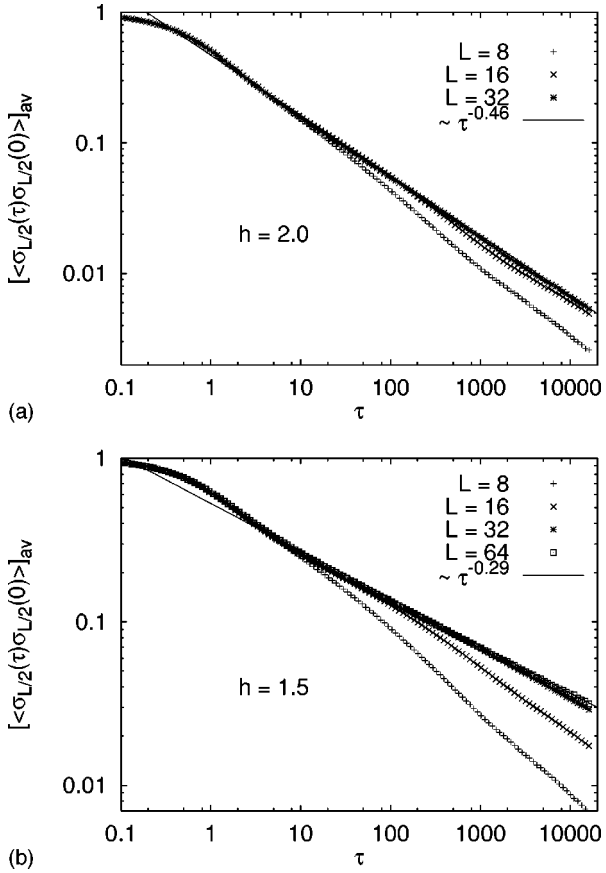

FIG. 11. The bulk autocorrelation function $[\langle \sigma^x_{L/2}(\tau)\sigma^x_{L/2}(0)\rangle]_{\rm av}$ in imaginary time in the disordered phase ($h>1$), calculated at a central spin $i=L/2$ with Eq. (2.23) via the Pfaffian method presented in Sec. II. The straight lines are fits to the expected power-law decay $\tau^{-1/z(h)}$.

VII. DISCUSSION

In this paper the critical and off-critical properties of the random transverse-field Ising spin chain are studied by analytical and numerical methods and by phenomenological scaling theory. The previously known exact,[7] RG,[2] and numerical results[11,30,31,12] about the model have been extended and completed here in several directions. The scaling behavior of the surface magnetization is obtained through a mapping to an adsorbing random walk and the critical exponents β_s, ν, and x^s_m are calculated exactly. We have also shown that the scaling behavior in the microcanonical ensemble is anomalous.

Using the correspondence between the surface magnetization and the adsorbing walks we have identified strongly coupled domains in the system, where the couplings have a surviving walk character, and estimated the distribution of low-energy excitations both in the critical and off-critical regions. This provides a comprehensive explanation of the microscopic origin of the Griffiths-McCoy singularities. It turns out that most of the astonishing features of the critical as well as the off-critical (Griffiths-McCoy) properties can be simply explained via random-walk analogies. However, one prediction by Fisher,[2] namely, the exact value of the bulk magnetization exponent β and its surprising relation to the golden mean, still lacks a *simple* explanation in terms of universal properties of random walks.

In the numerical part of our work we have treated relatively large ($L\leqslant 128$) finite systems. At the critical point we have calculated the magnetization profiles for different boundary conditions, which are found to follow accurately the conformal predictions, although the system is not conformally invariant. We have also increased the numerical accuracy in the calculation of the bulk magnetization scaling dimension. In the off-critical regions we have determined the dynamical exponent $z(\delta)$ from different physical quantities. The obtained results give support to the scaling prediction that the Griffiths-McCoy singularities are characterized by the single parameter $z(\delta)$. Here we note that the numerical

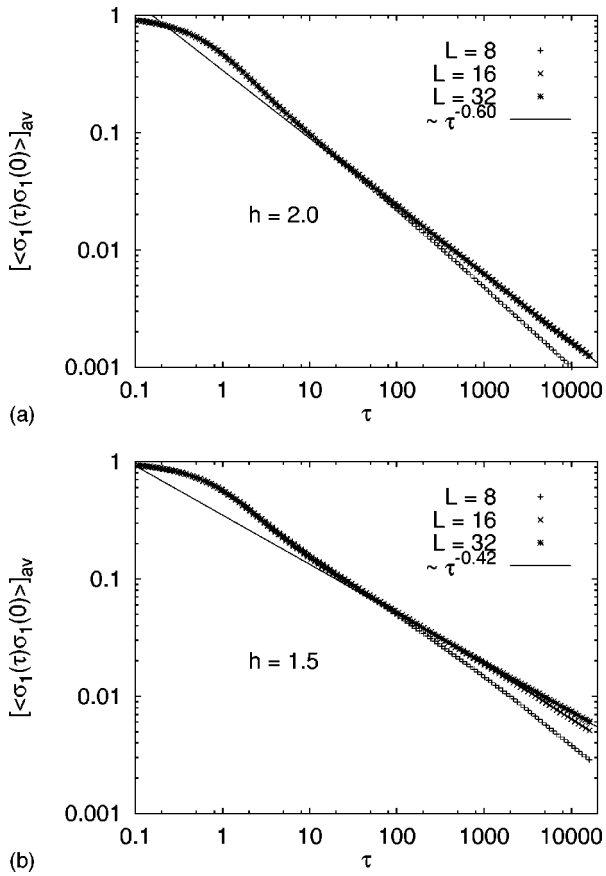

FIG. 12. The surface autocorrelation function $[\langle \sigma_1^x(\tau)\sigma_1^x(0)\rangle]_{\rm av}$ in imaginary time in the disordered phase ($h>1$), calculated via Eq. (2.21). The straight lines are fits to the expected power-law decay $\tau^{-1/z(h)}$.

data show systematic differences, when $z(\delta)$ is calculated from bulk or from surface quantities. A similar observation has been made in Ref. 12, too. The possible origin of the discrepancies is, that the SCD's, which are responsible for the Griffiths-McCoy singularities, have different environments at the surface and in the volume of the system. Then, from the argument leading to Eqs. (4.5), (4.6) one can obtain

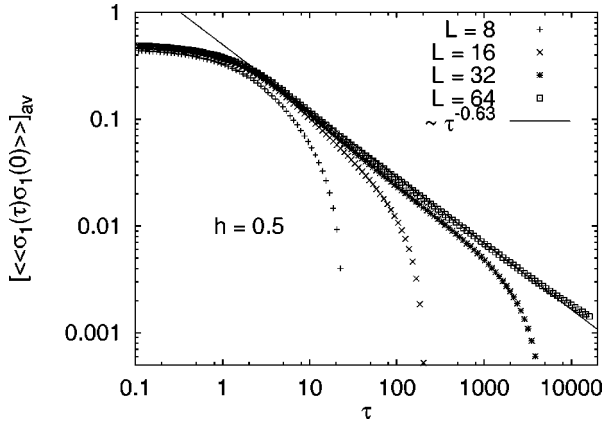

FIG. 13. The connected part of the surface autocorrelation function $[\langle\langle \sigma_1^x(\tau)\sigma_1^x(0)\rangle\rangle]_{\rm av}=[\langle \sigma_1^x(\tau)\sigma_1^x(0)\rangle - m_s^2]_{\rm av}$ in imaginary time in the ordered phase ($h<1$), calculated via Eq. (2.21), but now substracting $|\Phi_1(1)|^2$. The straight lines are fits to the expected power-law decay $\tau^{-1/z(h)}$.

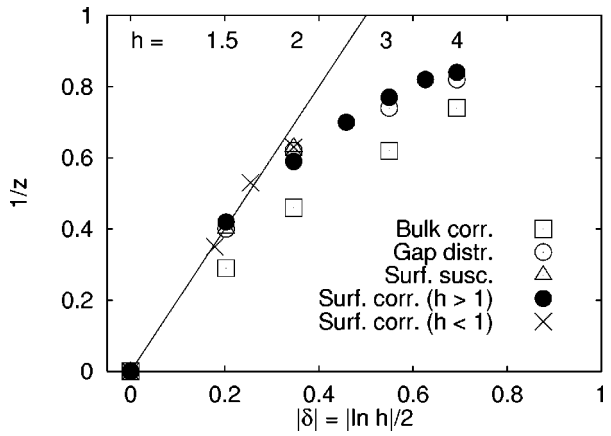

FIG. 14. Summary of all estimates of the dynamical exponent $z(h)$ as a function of the distance from the critical point $\delta = |\ln h|/2$. The open circles are the estimates from the gap distribution, as exemplified in Fig. 2, open triangles: surface susceptibility distribution (cf. Fig. 10), full circles: surface autocorrelation function (cf. Fig. 12), crosses: surface autocorrelation function in the ordered phase (cf. Fig. 13), open squares: bulk autocorrelation function (cf. Fig. 11). Note that whereas all former estimates agree within the error margin (which is roughly the size of the symbols) the latter estimate, namely the one obtained via the bulk autocorrelation function, differs significantly from all others.

logarithmic corrections between the dynamical exponents. This fact can then explain the differences in the finite-size data. We have numerically studied the Griffiths-McCoy singularities in the ferromagnetic phase, too. In this region the second gap of the Hamiltonian and the *connected* autocorrelation function scale with the dynamical exponent, which, according to numerical results, satisfies the duality relation.

ACKNOWLEDGMENTS

F.I.'s work has been supported by the Hungarian National Research Fund under Grants Nos. OTKA TO12830, OTKA TO23642, OTKA TO17485, and OTKA TO15786, and by the Ministery of Education under Grant No. FKFP 0765/1997. We are indebted to L. Turban for a critical reading of the manuscript. Useful discussions with T. Nieuwenhuizen, F. Pazmandi, G. Zimanyi, and A. P. Young are gratefully acknowledged. H.R.'s work was supported by the Deutsche Forschungsgemeinschaft (DFG) and he thanks the Aspen Center for Physics, the International Center of Theoretical Physics in Trieste, and the Research Institute for Solid State Physics, Budapest, where part of this work has been completed, for kind hospitality.

APPENDIX: ADSORBING RANDOM WALKS

Here we summarize the basic properties of one-dimensional random walks in the presence of an adsorbing wall. For simplicity, first we consider a walker, which makes steps of unit lengths with probabilities p and $q=1-p$ to the positive and to the negative directions, respectively. Starting at a distance $s>0$ from an adsorbing wall we are interested in the surviving probability $P_{\rm surv}(\delta_w,L)$ after L steps. Here

$$\delta_w = q - p \tag{A1}$$

measures the average drift of the walk in one step: for $\delta_w<0$ ($\delta_w>0$) the walk has a drift towards (off) the wall.

The probability $W_L(l)$, that the walker after L steps is at a position $l \leqslant L$, can be easily obtained by the mirror method:[32]

$$W_L(l)=p^{(L+l)/2}q^{(L-l)/2}\left(\frac{L!}{[(L+l)/2]![(L-l)2]!}-\frac{L!}{[(L+l)/2+s]![(L-l)/2-s]!}\right). \tag{A2}$$

In the following we take $s=1$ and in the limit $L \gg 1$, $l \gg 1$ we use the central limit theorem to write in the continuum approximation $l \to x$ and $W_L(l) \to P_L(x)$ as

$$P_L(x)=\frac{1}{p}\frac{x}{L}\frac{1}{\sqrt{2\pi L\sigma^2}}\exp\left[-\frac{(x-\overline{x})^2}{2L\sigma^2}\right] \tag{A3}$$

with

$$\overline{x}=(p-q)L=-\delta_w L, \quad \sigma^2=4pq. \tag{A4}$$

The surviving probability is then given by

$$P_{\rm surv}(\delta_w,L)=\int_0^\infty P_L(x)dx=\sqrt{\frac{2\sigma^2}{p^2\pi L}}\exp(-\overline{y}^2)\times\left\{\frac{1}{2}+\frac{\overline{y}}{2}\sqrt{\pi}\exp(\overline{y}^2)[1-\Phi(-\overline{y})]\right\}, \tag{A5}$$

where

$$\overline{y}=\frac{\overline{x}}{\sqrt{2L\sigma^2}}=-\delta_w\sqrt{\frac{L}{2\sigma^2}}, \tag{A6}$$

and $\Phi(z)=2/\sqrt{\pi}\int_0^z \exp(-t^2)dt$ is the error function.[33]

In the following we evaluate $P_{\rm surv}(\delta_w,L)$ in Eq. (A5) in the different limits. In the symmetric case $\delta_w=0$, $p=1/2$:

$$P_{\rm surv}(\delta_w=0,L)=\frac{1}{\sqrt{8\pi L}}\sim L^{-1/2}. \tag{A7}$$

For $\delta_w>0$, when $p<q$ and the walk has a drift towards the wall the surviving probability has an exponential decay as $\overline{y}\to-\infty$:

$$P_{\rm surv}(\delta_w>0,L)=\sqrt{\frac{2\sigma^2}{p^2\pi L}}\exp(-\overline{y}^2)\frac{1}{4\overline{y}^2}\sim L^{-1/2}\exp(-L/\xi_w)\xi_w/L, \tag{A8}$$

with a correlation length

$$\xi_w=\frac{2\sigma^2}{\delta_w^2}. \tag{A9}$$

Finally, for $\delta_w<0$, when $p<q$ and the walk is drifted from the wall the surviving probability has a finite limit:

$$P_{\rm surv}(\delta_w<0,L)=\sqrt{\frac{2\sigma^2}{p^2\pi L}}\overline{y}+\sqrt{\frac{2\sigma^2}{p^2\pi L}}\exp(-\overline{y}^2)\frac{1}{4\overline{y}^2}=-\frac{\delta_w}{p}+\sqrt{\frac{2\sigma^2}{p^2\pi L}}\exp(-L/\xi_w)\xi_w/L, \tag{A10}$$

which is approached exponentially.

The size of *transverse fluctuations* of the adsorbing walk is given by

$$l_{\rm tr}(\delta_w,L)=\int_0^\infty P_L(x)xdx/P_{\rm surv}(\delta_w,L), \tag{A11}$$

where

$$\int_0^\infty P_L(x)xdx=\frac{2\sigma^2}{p\sqrt{\pi}}\exp(-\overline{y}^2)\left\{\frac{\overline{y}}{2}+\frac{\sqrt{\pi}}{4}(2\overline{y}^2+1)\exp(\overline{y}^2)\times[1-\Phi(-\overline{y})]\right\}. \tag{A12}$$

In the symmetric limit $\delta_w=0$:

$$l_{\rm tr}(\delta_w=0,L)=\sqrt{8\pi L}\sim L^{1/2}. \tag{A13}$$

For $\delta_w>0$ the transverse fluctuations in leading order are independent of L:

$$l_{\rm tr}(\delta_w>0,L)=\frac{2\sigma^2}{\delta_w}, \tag{A14}$$

while for $\delta_w<0$, when there is a drift of the walk from the wall the transverse fluctuations grow linearly with L:

$$l_{\rm tr}(\delta_w<0,L)=\delta_w L. \tag{A15}$$

The *maximal value of the transverse fluctuations* $l_{\rm tr}^{\rm max}(\delta_w,L)$ for $\delta \leqslant 0$ are in the same order of magnitude as their average values in Eqs. (A13) and (A15). However for $\delta>0$ the maximal value is generally larger than the average one in Eq. (A14). In this case $l_{\rm tr}^{\rm max}(\delta_w>0,L)$ is determined by a *rare event*, in which a large fluctuation of positive steps is followed by a drift process towards the average behavior. If the number of steps in the drift process is αL, where $0<\alpha<1$, then

$$l_{\rm tr}^{\rm max}(\delta_w>0,L)=\alpha L\delta_w. \tag{A16}$$

[1] See, H. Rieger and A. P. Young, in *Complex Behavior of Glassy Systems*, edited by M. Rubi and C. Perez-Vicente, Lecture Notes in Physics Vol. 492 (Springer-Verlag, Heidelberg, 1997), p. 256, for a review.

[2] D. S. Fisher, Phys. Rev. Lett. **69**, 534 (1992); Phys. Rev. B **51**, 6411 (1995).

[3] S. Sachdev and T. Senthil, Phys. Rev. Lett. **77**, 5292 (1996).

[4] H. Rieger and N. Kawashima (unpublished); C. Pich and A. P. Young (unpublished); T. Ikegami, S. Miyashita, and H. Rieger, J. Phys. Soc. Jap. (to be published).

[5] R. B. Griffiths, Phys. Rev. Lett. **23**, 17 (1969).

[6] B. McCoy, Phys. Rev. Lett. **23**, 383 (1969).

[7] B. M. McCoy and T. T. Wu, Phys. Rev. **176**, 631 (1968); **188**, 982 (1969); B. M. McCoy, *ibid.* **188**, 1014 (1969).
[8] R. Shankar and G. Murthy, Phys. Rev. B **36**, 536 (1987).
[9] R. A. Hyman, K. Yang, R. N. Bhatt, and S. M. Girvin, Phys. Rev. Lett. **76**, 839 (1996).
[10] R. H. McKenzie, Phys. Rev. Lett. **77**, 4804 (1996).
[11] A. P. Young and H. Rieger, Phys. Rev. B **53**, 8486 (1996).
[12] A. P. Young, Phys. Rev. B **56**, 11 691 (1997).
[13] E. Lieb, T. Schultz, and D. Mattis, Ann. Phys. (N.Y.) **16**, 407 (1961); S. Katsura, Phys. Rev. **127**, 1508 (1962); P. Pfeuty, Ann. Phys. (Paris) **57**, 79 (1970).
[14] F. Iglói and L. Turban, Phys. Rev. Lett. **77**, 1206 (1996).
[15] In the eigenvalue problem in Eq. (2.2) the $\varepsilon_1=0$ eigenvalue is twofold degenerate, which corresponds to the fact that the $h_1=0$, $h_L\neq 0$ and the $h_1\neq 0$, $h_L=0$ boundary conditions are related through duality in Eq. (2.11), and the second eigenvector is given by $V_2(i)=\delta_{2L,i}$. In the fermionic problem in Eq. (2.1) we have just *one* zero mode, which is characterized by the first type of eigenvector above Eq. (2.9) for $h_L=0$. If one takes $h_1=0$ (and $h_L\neq 0$), then the zero-energy eigenvector is of the second type, i.e., $V_1(i)=\delta_{1,i}$, and the expectational value of the first spin from Eq. (2.7) is $\langle 0|\sigma_1^x|0\rangle=1$, as it should be.
[16] I. Peschel, Phys. Rev. B **30**, 6783 (1984).
[17] J. Stolze, A. Nöppert, and G. Müller, Phys. Rev. B **52**, 4319 (1995).
[18] The condition that the random walk does not go below the ''time'' axis corrresponds to the condition that two end spins of an effective spin cluster not be decimated in Fisher's RG treatmet (Ref. 2).
[19] B. M. McCoy and T. T. Wu, Phys. Rev. **162**, 436 (1967).
[20] The ''strongly coupled domains'' here are similar to the ''effective spin clusters'' in Fisher's RG treatment (Ref. 2).
[21] F. Iglói, L. Turban, D. Karevski, and F. Szalma, Phys. Rev. B **56**, 11 031 (1997).
[22] F. Iglói, D. Karevski, and H. Rieger, Eur. Phys. J. B **1**, 513 (1998).
[23] F. Pázmándi, R. T. Scalettar, and G. T. Zimányi, Phys. Rev. Lett. **79**, 5130 (1997).
[24] J. T. Chayes, L. Chayes, D. S. Fisher, and T. Spencer, Phys. Rev. Lett. **57**, 2999 (1986).
[25] M. E. Fisher, in *Renormalization Group in Critical Phenomena and Quantum Field Theory*, edited by J. D. Gunton and M. S. Green (Temple University, Philadelphia, 1974), p. 65; F. Iglói and L. Turban, Phys. Rev. B **47**, 3404 (1993).
[26] C. de Calan, J. M. Luck, T. M. Nieuwenhuizen, and D. Petritis, J. Phys. A **18**, 501 (1985); T. M. Nieuwenhuizen and M. C. W. van Rossum, Phys. Lett. A **160**, 461 (1991). Note that in these works the distribution of a random variable $z=1+x_1+x_1x_2+x_1x_2x_3+\cdots$ with random uncorrelated x_i has been studied, which is identical to our variable m_s^{-2}.
[27] F. Iglói, I. Peschel, and L. Turban, Adv. Phys. **42**, 683 (1993).
[28] M. E. Fisher and P.-G. De Gennes, C. R. Seances Acad. Sci., Ser. B **287**, 207 (1978).
[29] L. Turban and F. Iglói, J. Phys. A **30**, L105 (1997).
[30] F. Iglói and H. Rieger, Phys. Rev. Lett. **78**, 2473 (1997).
[31] H. Rieger and F. Iglói, Europhys. Lett. **39**, 135 (1997).
[32] See, e.g., R. K. Pathria, *Statistical Mechanics* (Pergamon, Oxford, 1972).
[33] I. S. Gradshteyn and I. M. Ryzhik, *Table of Integrals, Series, and Products* (Academic, London, 1980).